J Fluoresc (2014) 24:1563–1570
DOI 10.1007/s10895-014-1438-4

ORIGINAL PAPER

The Amidine Based Colorimetric Sensor for Fe^{3+}, Fe^{2+}, and Cu^{2+} in Aqueous Medium

Jitendra Nandre · Samadhan Patil · Prashant Patil · Suban Sahoo · Carl Redshaw · Pramod Mahulikar · Umesh Patil

Received: 19 May 2014 / Accepted: 11 August 2014 / Published online: 12 September 2014

Abstract An amidine based chemosensor **AM-1** was synthesized and characterized by various spectroscopic (FT-IR, ^{1}H-NMR and mass) data and elemental analyses. Sensor **AM-1** exhibited high selectivity and sensitivity towards Fe^{3+}, Fe^{2+} and Cu^{2+} in the presence of other surveyed ions (such as Sr^{2+}, Cr^{3+}, Co^{2+}, Ni^{2+}, Zn^{2+}, Ag^{+}, Al^{3+}, Ba^{2+}, Ca^{2+}, Cd^{2+}, Cs^{+}, Hg^{2+}, K^{+}, Li^{+}, Mg^{2+}, Mn^{2+}, Na^{+} and Pb^{2+}) with a distinct naked-eye detectable color change and a shift in the absorption band. Moreover, the emission of **AM-1** was quenched selectively only in the presence of Fe^{3+}.

Keywords Amidine · Chemosensor · Chromogenic receptor · Multi metal ion sensor · DFT

Electronic supplementary material The online version of this article (doi:10.1007/s10895-014-1438-4) contains supplementary material, which is available to authorized users.

J. Nandre · S. Patil · P. Patil · P. Mahulikar (✉) · U. Patil (✉)
School of Chemical Sciences, North Maharashtra University, Jalgaon 425 001, India
e-mail: mahulikarpp@rediffmail.com
e-mail: udpatil.nmu@gmail.com

P. Patil
S.S.V.P.S's L. K. Dr. P. R. Ghogrey Science College, Dhule 424 001, India

S. Sahoo
Department of Applied Chemistry, S. V. National Institute Technology, Surat 395 007, Gujrat, India

C. Redshaw
Department of Chemistry, University of Hull, Cottingham Road, Hull HU6 7RX, UK

Introduction

Chemosensors are molecules of abiotic origin that reveal a significant change in the electronic, magnetic or optical signals when interacted with a specific guest/s (ions/molecules) [1, 2]. Among the various chemosensing systems, sensors based on a naked-eye response (colorimetric) have many advantages because of their ability to provide a simple, sensitive, selective, precise and economical method for the detection of a target analyte without the use of specific/sophisticated instrumentation [3–6]. In colorimetric chemosensors, the spectral and visual color changes i.e. the responses obtained at the molecular level in solution opened the door for the qualitative and quantitative determination of the target analyte.

Recently, the design and synthesis of selective and sensitive chemosensors for the selective detection of transition metal ions has gained enormous attention because of their participation in a variety of fundamental biological and physiological processes including in human metabolic processes [7–10]. As important physiologically associated metal ions, both the Fe^{2+} and Fe^{3+} ions play an indispensable role in many biochemical processes at the cellular level. Numerous enzymes use iron ions as a catalyst for electron transfer, oxygen metabolism, and RNA and DNA synthesis [11, 12]. However, both its deficiency (hypoferremia) and excess (hyperferremia) can induced a variety of diseases. Several serious diseases such as Alzheimer, Parkinson's and Huntington's disease etc. known to occur due to the cellular toxicity caused by iron ions [13, 14]. Similarly, Cu^{2+} is a major metal pollutant because of its widespread use [15]. Cu^{2+} ions play an important role as a catalytic cofactor in a variety of metallo-enzymes, including superoxide dismutase, cytochrome *c* oxidase, and tyrosinase [16]. Cu^{2+} also exhibits toxicity allied with neurological diseases such as Alzheimer's, Wilson's and prion disease [17–20]. Due to the biological importance of Cu^{2+}, Fe^{2+},and

Fe^{3+} ions, a method for the rapid, selective and sensitive recognition of these ions in food, pharmaceutical products and biological samples such as blood, urine, etc. is of great significance.

As a result, intense research has been focused on the development of sensitive and selective receptors for the qualitative and quantitative recognition of Cu^{2+}, Fe^{2+},and Fe^{3+}. Interestingly, as summarized in Table S1, the various reported sensors are quite specific, either for Cu^{2+} or Fe^{2+} or Fe^{3+}, or for Cu^{2+} and Fe^{3+}, or for Fe^{2+} and Fe^{3+} [4, 5, 21–30], but to the best of our knowledge, a colorimetric chemosensor for the simultaneous detection of Cu^{2+}, Fe^{2+} and Fe^{3+} ions remains unreported. Herein, as a part of our efforts in the field of analyte recognition [11, 29–33], the chemosensor **AM-1** has been developed for the selective and sensitive detection of Cu^{2+}, Fe^{2+} and Fe^{3+} ions in aqueous medium. The cation recognition ability of **AM-1** towards different metal ions was studied by experimental (naked-eye, UV-visible, and fluorescence spectroscopy) and theoretical methods. Obtained results in naked eye study have successfully applied the receptor **AM-1** as an indicator for the 'in situ' qualitative detection of Fe^{3+}, Fe^{2+} and Cu^{2+}. Interestingly, the fluorescence of receptor **AM-1** was quenched selectively in the presence of Fe^{3+} among the other tested metal ions including Fe^{2+} and Cu^{2+}.

Results and Discussion

The receptor **AM-1** was efficiently synthesized by the reaction of 2-cyanopyridine and 4-bromoaniline in the presence of $TiCl_4$ (Scheme 1) [34]. The molecular structure of **AM-1** was established by various spectroscopic (FT-IR, ^{1}HNMR and mass) data and elemental analyses (Fig. S1–3). The recognition ability of **AM-1** towards different metal ions was studied by naked eye, UV-visible and fluorescence spectroscopy. The obtained results were supported by theoretical study.

UV–Vis Study

The UV–Vis absorption spectra of the receptor **AM-1** (5×10^{-5} M, in methanol) was studied in the absence and presence of 5 equivalents of different metal ions such as Sr^{2+}, Cr^{3+}, Co^{2+}, Ni^{2+}, Zn^{2+}, Ag^{+}, Al^{3+}, Ba^{2+}, Ca^{2+}, Cd^{2+}, Cs^{+}, Hg^{2+}, K^{+}, Li^{+}, Mg^{2+}, Mn^{2+}, Na^{+}, Pb^{2+}, Cu^{2+}, $Fe^{2+}$and Fe^{3+} (1×10^{-2} M, in water). Receptor **AM-1** exhibited two absorption bands at 225 and 272 nm. Upon addition of Fe^{3+} ions to the solution of **AM-1**, a hypochromic shift was observed at 225 nm while a blue shift of 6 nm was observed at 272 nm with the appearance of a new broad charge transfer band between 350 and 450 nm. The charge transfer band of lower intensity was also observed in the presence Cu^{2+} and Fe^{2+} (Fig. 1). The spectral changes associated with **AM-1** can be attributed to the intermolecular charge transfer (ICT) process occurred due to the delocalization of electrons from the imine nitrogen (C=N) of the amidine to the metal ions during complexation. However, no significant changes in the absorption spectrum of **AM-1** were observed with other metal ions, there by revealing the selectivity towards Cu^{2+}, Fe^{2+} and Fe^{3+}.

The absorption titrations of **AM-1** with the metal ions (Cu^{2+}, Fe^{2+}, and Fe^{3+}) were next performed to examine the recognition ability. As shown in Fig. 2, on successive addition of incremental amounts of Fe^{3+} to the **AM-1** solution, the receptor bands were gradually shifted with the appearance of a new charge transfer band. Using the absorption titration data, the binding constant of 5×10^{3} M^{-1} was calculated for Fe^{3+} from the Benesi-Hildebrand Plot (Fig. S4). The detection and quantification limits of 0.6 and 1.9 μM, respectively for Fe^{3+} were estimated (Fig. S5). Similarly, the binding constants of 5.2×10^{3} M^{-1} and 9.7×10^{2} M^{-1} were calculated for the metal ions Cu^{2+} and Fe^{2+} respectively from the Benesi-Hildebrand Plots (Fig. S6–7).

The binding stoichiometry for **AM-1**.Fe^{3+}, **AM-1**.Fe^{2+} and **AM-1**.Cu^{2+} complexes were calculated by plotting the Job's plot between the mole fractions of Fe^{3+}, Fe^{2+} and Cu^{2+} with the absorption changes at 267 nm (Fig. 3). The maximum was obtained at a molar fraction of 0.5, which clearly delineated the formation of a ferric complex in 1:1 stoichiometry. Further, the stable **AM-1**.Fe^{2+} and **AM-1**.Cu^{2+} complexes were synthesized and characterized by LC-MS. The proposed 1:1 stoichiometry for both **AM-1**.Fe^{2+} and **AM-1**.Cu^{2+} complexes was supported by the obtained mass data (Fig. S8–9).

Colorimetric (Naked Eye) Study

In colorimetric experiments, significant color changes of the **AM-1** solutions were observed upon addition of Fe^{3+}, Fe^{2+}, and Cu^{2+} over the other tested metal ions (Fig. 4). A distinct color change of **AM-1** from colorless to red, orange and green was observed in the presence of Fe^{2+}, Fe^{3+} and Cu^{2+} ions respectively, which indicates the sensitive and selective 'naked-eye' detecting ability for these cations. By utilizing the benefits of the 'naked-eye' results, we have applied the receptor **AM-1** as an indicator for the 'in situ' qualitative detection of Fe^{3+}, Fe^{2+} and Cu^{2+} (Fig. 5). A solution of receptor **AM-1** (3 mL, 1×10^{-3} M, in methanol) is colorless. After addition of 1 equivalent of Fe^{2+}, it turns into dark blood red color. When

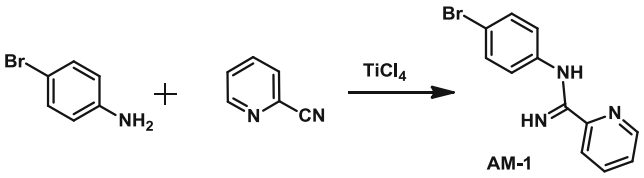

Scheme 1 Synthesis of receptor **AM-1**

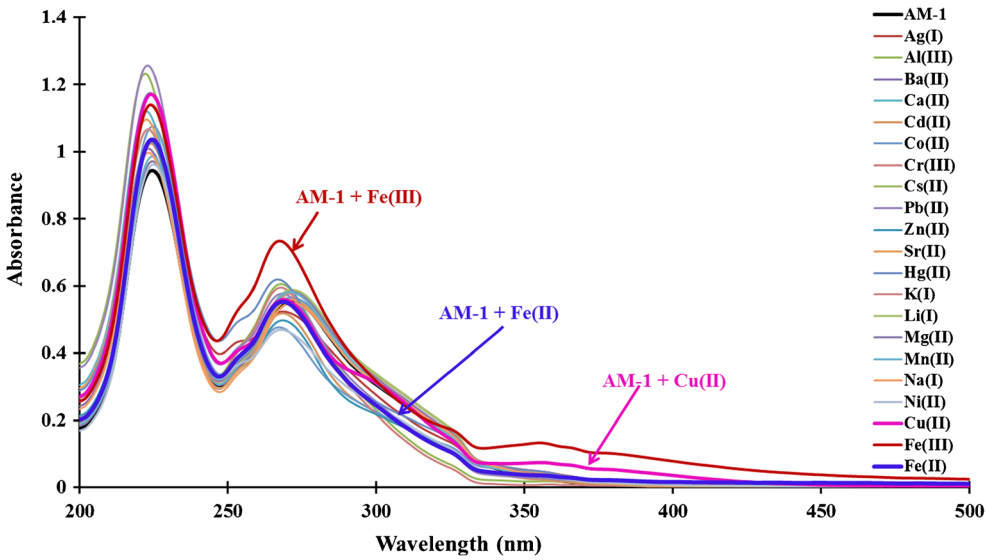

Fig. 1 Absorbance spectral changes of **AM-1** (2 mL, 5×10^{-5} M, in methanol) upon addition of 5 equivalents of various metal ions (50 μL, 1×10^{-2} M, in water)

0.1 M $K_2Cr_2O_7$ solution was added to this red color solution, immediate color change from dark red to faint yellow was observed which supports the conversion of Fe^{2+} into Fe^{3+}. On further addition of 0.1 M $NaBH_4$, the observed faint yellow color was converted reversibly into a dark red color. Further, the colorless solution of **AM-1** was reappeared with the excess addition of $NaBH_4$. These results inferred that we can monitored the presence of both the oxidation states of iron (Fe^{2+} and Fe^{3+}) by using the receptor **AM-1**. In another experiment, we have added copper powder to the colorless solution of receptor **AM-1**. To this colorless mixture, addition of 0.1 M $AgNO_3$ solution resulted in a remarkable color change from colorless to green, which indicates the conversion of metallic copper into the Cu^{2+} state. Moreover, it is interesting to mention here that all three ions (Fe^{2+}, Fe^{2+} and Cu^{2+}) shows reversibility in the color change on addition of aq. EDTA solution. The above naked-eye results opens the door for the applications of **AM-1** for the 'in situ' qualitative determination of three ions, namely Fe^{3+}, Fe^{2+} and Cu^{2+}.

Fluorescence Study

The cation binding behavior of **AM-1** was also investigated by emission measurements. Addition of Fe^{3+} ions (5 equivalents, 50 μL, 1×10^{-2} M, in water) to the **AM-1** solution (2 mL, 5×10^{-5} M) in methanol results in a distinct fluorescence quenching (Fig. 6). However, in the presence of other metal ions such as Fe^{2+}, Cu^{2+}, Sr^{2+}, Cr^{3+}, Co^{2+}, Ni^{2+}, Zn^{2+}, Ag^{+}, Al^{3+}, Ba^{2+}, Ca^{2+}, Cd^{2+}, Cs^{+}, Hg^{2+}, K^{+}, Li^{+}, Mg^{2+}, Mn^{2+}, Na^{+} and Pb^{2+}, the fluorescence intensity of **AM-1** at 305 nm either did not induced any significant changes or was slightly enhanced under identical conditions. In another experiment, the Fe^{3+} sensing ability of **AM-1** under a competition environment was investigated in the presence of potentially interfering metal ions by fluorescence measurements (Fig. S10). For methanol solutions of **AM-1**, addition of 2 equiv. of Fe^{3+} in the presence of 2 equiv. of other tested metal ions caused a dramatic quenching in the fluorescence intensity of **AM-1** with either very slight or no interference effects. Therefore,

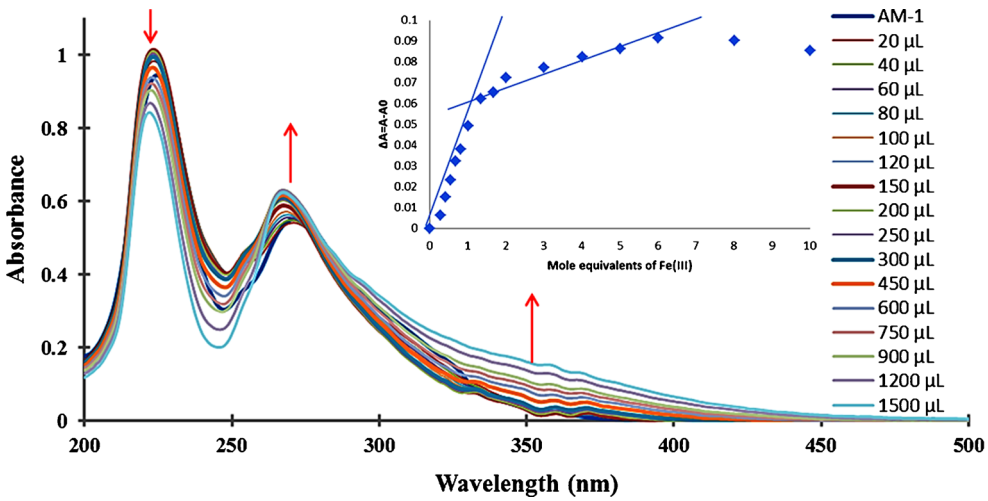

Fig. 2 Absorption spectral changes of **AM-1** (3 mL, 5×10^{-5} M, in methanol) upon addition of 0–10 equivalents of Fe^{3+}ions (0–1,500 μL, 1×10^{-3} M, in water). *Inset*: mole ratio plot from absorption titration of **AM-1** with Fe^{3+}

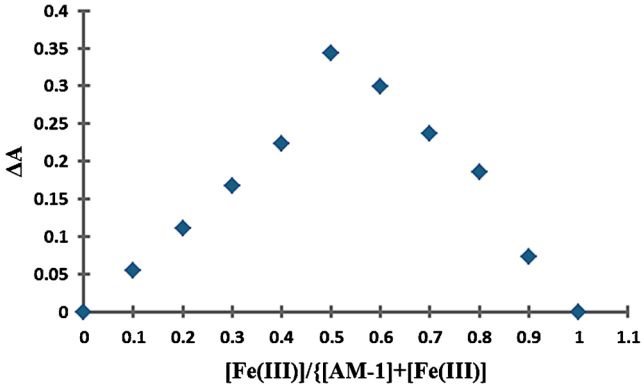

Fig. 3 Jobs Plot for **AM-1** and Fe^{3+}, indicating the formation of a 1:1 (L:M) complex

it can be concluded that **AM-1** is a reliable, highly selective and sensitive turn-off fluorescent sensor for Fe^{3+}.

The fluorescence titration of **AM-1** (2 mL, 5×10^{-5} M, in methanol) with Fe^{3+} (1×10^{-3} M, in water) was performed via the successive addition of incremental concentrations of Fe^{3+} (0–1,000 μL). The fluorescence intensity of **AM-1** was gradually quenched at 305 nm (Fig. 7). Based on the fluorescence titration data, the detection and quantification limits of 14 and 41 μM, respectively for Fe^{3+} were estimated (Fig. S11). Also, the binding constant (*K*) of **AM-1** with Fe^{3+} was determined by a Benesi-Hildebrand plot (Fig. S12) and a Scatchard plot (Fig. S13) from the fluorescence titration data. The binding affinity of **AM-1** was found to be $\approx1\times10^{5}$ M^{-1} for Fe^{3+}.

The quenching process can be mathematically expressed by the Stern–Volmer Eq. (1), which allows us to determine the types of quenching. If the Stern–Volmer plot is linear then the quenching is of a static type rather than dynamic quenching [35, 36].

$$F_0/F = 1 + k_q\tau_0[Q = 1 + K_{sv}[Q] \quad (1)$$

Where, F_0 and F are the fluorescence intensities in the absence and presence of the quencher, k_q is the bimolecular quenching constant, τ_0 is the lifetime of the fluorescence in the absence of the quencher, [Q] is the concentration of the quencher, and K_{sv} is the Stern–Volmer quenching constant. In the presence of a quencher, the fluorescence intensity is reduced from F_0 to F. Therefore, the ratio (F_0/F) is directly proportional to the quencher concentration [Q]. According to Eq. (1), the Stern–Volmer plot of F_0/F versus [Q] shows a linear graph with a slope of K_{sv} (Fig. 8). The linear Stern–Volmer plot indicates that the quenching is static for the **AM-1**.Fe^{3+} system [35]. The results also confirmed the formation of only one type of complex between the receptor **AM-1** and the Fe^{3+} ions.

Fig. 5 'In situ' qualitative detection of Fe^{3+}, Fe^{2+}, and Cu^{2+}

Computational Study

In the absence of a suitable single crystal of **AM-1** and its complexes, and to get more insight into the above experimental observations, DFT calculations were performed to understand the electronic environment and the changes in the structure of **AM-1** upon complexation with Fe^{3+}, Fe^{2+} and Cu^{2+}. During the computational study, two stable conformations of **AM-1** (L and L′) were optimized (Fig. 9). The form L is relatively more stable than L′ by 5.01 kcal/mol. There is an intramolecular H-bond (2.036 Å) between the amine proton (H6) with the pyridine-N atom. Also, the ligand exhibited two possible coordination modes (Fig. 10, mode I: Py-N and =NH and mode II: Py-N and -NH) forming a five-membered cheated ring with the metal ions. According to the calculated relative energy, the complexes preferred to coordinate through the Py-N and =NH. The Cu^{2+}, Fe^{2+} and Fe^{3+} complexes with the coordination mode I is relatively more stable than mode II by 25.15, 7.36 and 54.32 kcal/mol, respectively. In coordination mode I, the interaction energy was calculated by applying the equation [$E_{int} = E_{(ML)} - E_{(L)} - E_{(M)}$]. The E_{int} for the **AM-1.**Fe^{3+}, **AM-1.**Fe^{2+} and **AM-1.**Cu^{2+} complexes are −792.58, −286.83 and −330.29 kcal/mol, respectively. This result

Fig. 4 Photo of the vials containing **AM-1** (3 mL, 1×10^{-3} M, in methanol) in the presence of various metal ions (300 μL, 1×10^{-2} M, in water)

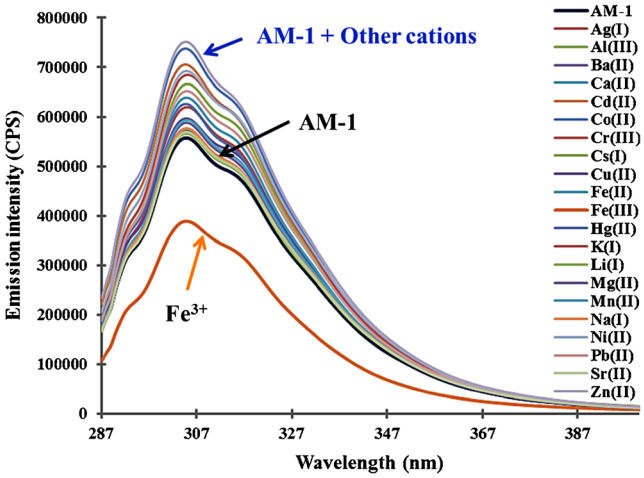

Fig. 6 Fluorescence spectral (λ_{ex}=277 nm) changes of **AM-1** (5×10^{-5} M, in methanol) upon addition of 5 equivalent of various metal ions (1×10^{-2} M, in water)

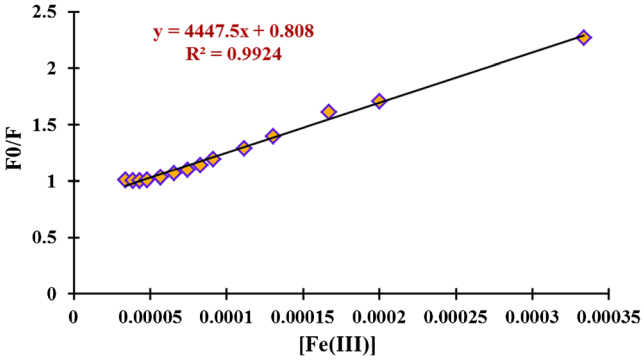

Fig. 8 Stern-Volmer Quenching Plot for Fe^{3+} with receptor **AM-1**

indicates that Fe^{3+} is forming a stronger complex with **AM-1** followed by Cu^{2+} and then Fe^{2+}.

The plots of the frontier molecular orbital's (FMO's) of **AM-1** and its complexes with Fe^{3+}, Cu^{2+} and Fe^{2+} were analyzed. As shown in Fig. S14 and S15, the electron density of the highest-occupied molecular orbital (HOMO) and lowest-unoccupied molecular orbital (LUMO) of the receptor located in two different rings suggests a strong intramolecular charge transfer. On complexation, the lowering of the band gap indicates the shift in the absorption band, and simultaneously the HOMO and LUMO indicates the formation of a charge-transfer complex between the receptor and metal ions.

Experimental

Materials and Methods

All the starting reagents and metal perchlorates were purchased either from S. D. Fine chemicals or Sigma Aldrich depending on their availability. All the reagents were used as received. All the solvents were of spectroscopic grade and were used without further treatment. The purity of the compounds and the progress of reactions were determined and

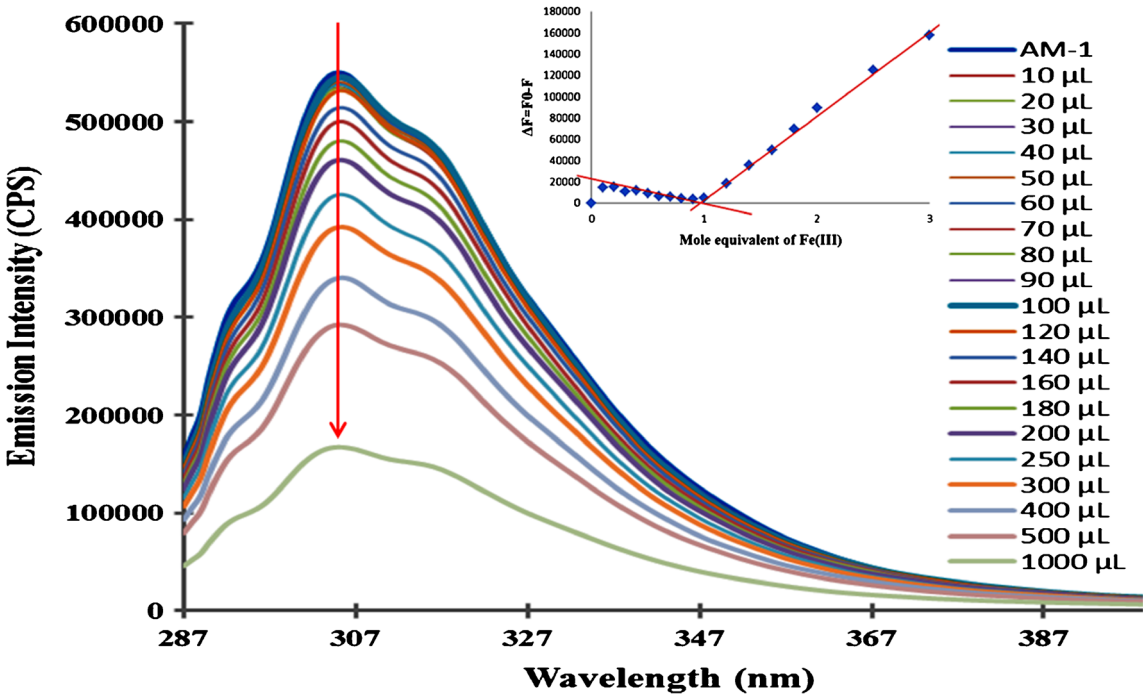

Fig. 7 Fluorescence spectral changes of sensor **AM-1** (2 mL, 5×10^{-5} M, in methanol) upon addition of 0–10 equivalents of Fe^{3+} (0–1,000 µL, 1×10^{-3} M, in water) at λ_{ex}=277 nm. *Inset*: mole ratio plot from fluorescence titration of **AM-1** with Fe^{3+}

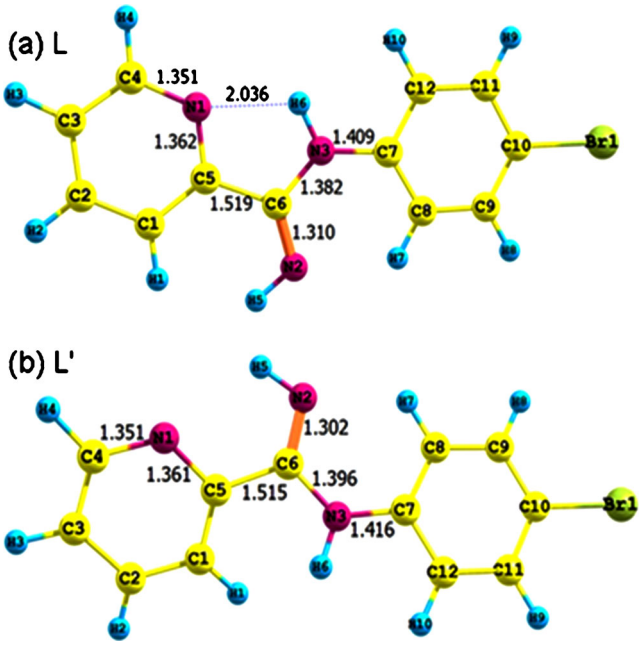

Fig. 9 Optimized structure of the two probable conformations (L and L′) of **AM-1** at B3LYP/SDD method

monitored by means of analytical thin layer chromatography (TLC). Pre-coated silica gel 60 F_{254} (Merck) on alumina plates (7×3 cm) were used and visualized by using either an iodine chamber or a short UV-Visible lamp. Melting points were recorded on the Celsius scale by open capillary method and are uncorrected. IR spectra were recorded on a Perkin-Elmer Spectrum One FT-IR spectrometer as potassium bromide pellets and nujol mulls, unless otherwise mentioned. NMR spectra were recorded in $CDCl_3$ on a Varian (Mercury Vx) SWBB Multinuclear probe spectrometer, operating at 300 and 75 MHz for ^{1}H NMR and ^{13}C NMR, respectively and shifts are given in ppm downfield from tetramethylsilane (TMS) as an internal standard. UV–Vis spectra were recorded on a U-3900 spectrophotometer (Perkine Elmer Co., USA) with a quartz cuvette (path length=1 cm). Fluorescence spectra were recorded on a Fluoromax-4 spectrofluorometer (HORIBA Jobin Yvon Co., France).

Synthesis of **AM-1**

In 250 ml dry round bottom flask, a mixture of 4-bromoaniline (1.28 g, 10 mmol) and 2-cyanopyridine (1.04 g, 10 mmol) was heated in an oil bath at a temperature range of 110–120 °C with constant stirring. After 30 min., $TiCl_4$ (1.33 ml, 12 mmol) was added to the flask. Then, the temperature was increased to 150–160 °C, and heating was continued for 3–4 h. The progress of reaction was monitored by TLC. After completion of the reaction, the obtained solid was cooled to room temperature and dissolved in a hot water followed by the solution was made alkaline with 10 % NaOH solution. This alkaline solution was extracted with dichloromethane [3×50 mL]. The organic layer was decolorized with activated charcoal and dried over anhydrous Na_2SO_4. After evaporating the solvent under reduced pressure, the crude amidine was obtained. This crude amidine was recrystallized from an acetone:hexane [10:90] system, to afford pure amidine. Yield: 2.24 g (81 %).

IR [KBr, cm^{-1}]: 3,376, 2,854, 1,640, 1,577, 1,530, 1,459, 1,377, 1,321, 1,300, 1,260, 1,151, 1,119, 1,096, 1,006, 818, 769, 722, 541. **LCMS [ESI, e/z (%)] :** 278 (100), 276 (100), 260 (20), 259 (20). **^{1}H NMR [$CDCl_3$, 300 MHz]:** 5.85 (br s, 2H, NH, C=NH), 6.88–6.91 (d, J=8.7 Hz, 2H, ArH), 7.38–7.50 (m, 3H, ArH), 7.79–7.84 (m, 1H, ArH), 8.36–8.39 (d, J= 8.1 Hz, 1H, ArH), 8.56–8.58 (m, 1H, ArH). Anal. calcd for

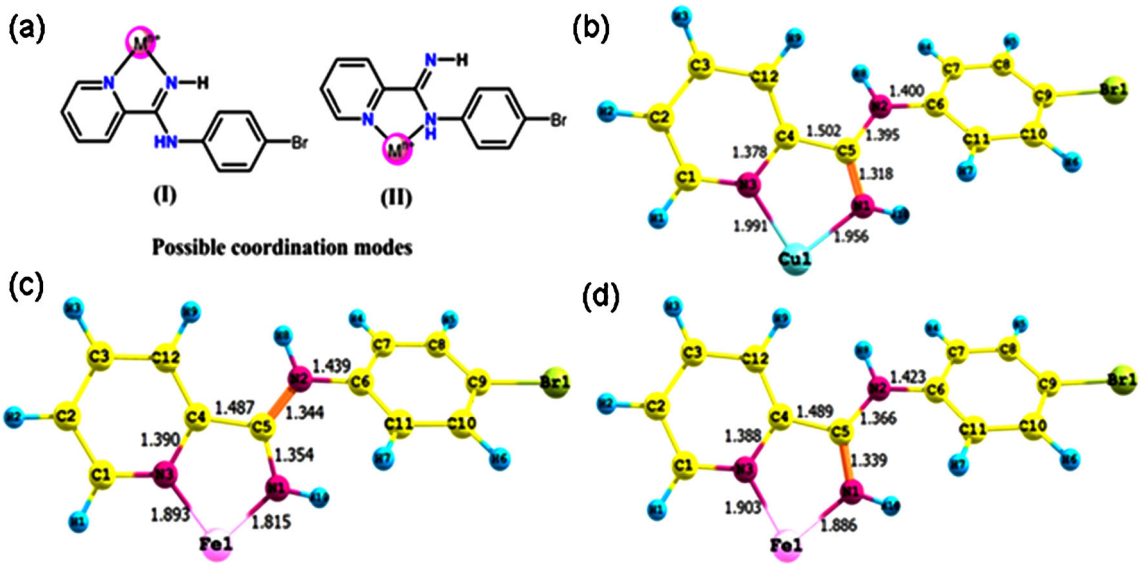

Fig. 10 **a** The possible coordination modes of **AM-1**, and the favorable optimized structure of the complexes **b AM-1.**Cu^{2+}, **c AM-1.**Fe^{2+} and **d AM-1.**Fe^{3+} at B3LYP/SDD method [36]

$C_{12}H_{10}BrN_3$: C, 52.20; H, 3.65; N, 15.22. Found: C, 52.54; H, 3.60; N, 15.28.

Spectroscopic Study

The aqueous stock solutions of cations of concentration 1×10^{-2} mol L^{-1} were prepared from their corresponding salt i.e. $AgClO_4$, $Al(ClO_4)_3.9H_2O$, $Ba(ClO_4)_2$, $Ca(NO_3)_2.4H_2O$, $Cd(ClO_4)_2.H_2O$, $Co(ClO_4)_2.6H_2O$, $Cr(ClO_4)_3.6H_2O$, $Fe(ClO_4)_2.xH_2O$, $HgCl_2$, LiBr, $Mg(ClO_4)_2$, $Mn(ClO_4)_2.H_2O$, $Ni(ClO_4)_2.6H_2O$, $Fe(ClO_4)_3.H_2O$, $Pb(ClO_4)_2.3H_2O$, $Zn(ClO_4)_2.6H_2O$, $Cu(ClO_4)_2.6H_2O$, respectively. The stock solution of **AM-1** (1×10^{-3} molL^{-1}) was prepared by dissolving an accurately weighed **AM-1** in CH_3OH and then diluted to 5×10^{-5} molL^{-1} with CH_3OH. These solutions were used for all spectroscopic studies after appropriate dilution. For spectroscopic titrations, the required amount of the diluted receptor **AM-1** was taken directly into a cuvette and the spectra were recorded after successive addition of the cations by using a micropipette.

Computational Analysis

The structural optimization of the receptor and its complexes with the metal ions (Cu^{2+}, Fe^{2+} and Fe^{3+}) was performed by applying the density functional theory (DFT) method in the gas phase by using the computer program Gaussian 09W [36]. All DFT calculations were performed with a hybrid functional B3LYP (Becke's three parameter hybrid functional using the LYP correlation functional) using the basis sets SDD. Then, the optimized geometries have been confirmed by frequency analyses at the same level of theory to ascertain the optimized structure were stable.

Conclusion

In summary, we have developed an easy-to-synthesize amidine based receptor **AM-1** for the selective detection of Fe^{2+}, Fe^{3+} and Cu^{2+} ions by colorimetric and UV–Vis spectral changes. The 1:1 binding stoichiometry for the **AM-1**.Fe^{3+}, **AM-1**.Fe^{2+}, and **AM-1**.Cu^{2+} complexes was proposed by Job's plot and LC-MS analysis. Interestingly, the receptor exhibited a highly selective and sensitive fluoresce turn-off response only in the presence of Fe^{3+}. Based on the spectral responses, the detection and quantification limits for receptor **AM-1** for Fe^{3+} were estimated at 0.6 and 1.9 μM, respectively from absorption measurements, whereas values of 14 and 41 μM, respectively were obtained from emission measurements. The sensor **AM-1** opens the door for the applications of **AM-1** for the 'in situ' qualitative determination of three ions, namely Fe^{3+}, Fe^{2+} and Cu^{2+}. The receptor **AM-1** with its' low cost, ease of preparation and impressive selectivity inferred that this approach could potentially lead to many more sensors being designed using the amidine moiety as a core skeleton.

Acknowledgments The author Dr. U. D. Patil is grateful to Department of Science & Technology, New Delhi, INDIA (Reg. No. CS-088/2013) and 'North Maharashtra University, Jalgaon', VCRMS Scheme, for the financial support.

References

1. Bell TW, Hext NM (2004) Supramolecular optical chemosensors for organic analytes. Chem Soc Rev 33:589–598
2. Suksai C, Tuntulani T (2003) Luminescent chemodosimeters for bioimaging. Chem Soc Rev 32:192–202
3. Kuan Z, Yue LC, Ping HL, Fang L (2010) Chromo-chemodosimetric detection for Fe^{2+} by Fenton reagent-induced chromophore-decolorizing of halogenated phenolsulfonphthale in derivatives. Sci China Chem 53:1398–1405
4. Liang ZQ, Wang CX, Yang JX, Gao HW, Tian YP, Tao XT, Jiang MH (2007) A highly selective colorimetric chemosensor for detecting the respective amounts of iron(II) and iron(III) ions in water. New J Chem 31:906–910
5. Sen S, Sarkar S, Chattopadhyay B, Moirangthem A, Basu A, Dharad K, Chattopadhyay P (2012) A ratiometric fluorescent chemosensor for iron: discrimination of Fe^{2+} and Fe^{3+} and living cell application. Analyst 137:3335–3342
6. Bhalla V, Arora H, Kumar M (2013) Aggregates of a triphenylene based chemosensing ensemble for sensitive detection of cyanide ions in an aqueous medium. Dalton Trans 42:4450–4455
7. Silva AP, Gunaratne HQN, Gunnlaugsson T, Huxley AJM, McCoy CP, Rademacher JT, Rice TE (1997) Signaling recognition events with fluorescent sensors and switches. Chem Rev 97:1515–1566
8. Valeur B, Leray I (2000) Design principles of fluorescent molecular sensors for cation recognition. Coord Chem Rev 205:3–40
9. Silva AP, McCaughan B, McKinney BOF, Querol M (2003) Newer optical-based molecular devices from older coordination chemistry. Dalton Trans 10:1902–1913
10. Callan JF, Silva AP, Magri DC (2005) Luminescent sensors and switches in the early 21st century. Tetrahedron 61:8551–8588
11. Sahoo SK, Sharma D, Bera RK, Crisponi G, Callan JF (2012) Iron(III) selective molecular and supramolecular fluorescent probes. Chem Soc Rev 41:7195–7227
12. Crabtree RH (1994) Metal ions at work. Science 266:1591–1592
13. Burdo JR, Connor JR (2003) Brain iron uptake and homeostatic mechanisms: an overview. BioMetals 16:63–75
14. Pithadia AS, Lee MH (2012) Metal-associated amyloid-β species in Alzheimer's disease. Curr Opin Chem Biol 16:67–73
15. High B, Bruce D, Richter MM (2001) Determining copper ions in water using electrochemilumincenec. Anal Chim Acta 449:17–22
16. Zhang LZ, Wang LY, Fan JL, Guo KX, Peng XJ (2011) A highly selective, fluorescent chemosensor for bioimaging of Fe^{3+}. Bioorg Med Chem Lett 21:5413–5416
17. Brewer GJ (2008) Overview of the role of copper in neurodegenerative diseases and potential treatment with tetrathiomolybdate. Cell Biol Toxicol 24:423–426
18. Barnham KJ, Bush AI (2008) Metals in Alzheimer's and Parkinson's diseases. Curr Opin Chem Biol 12:222–228
19. Li ZX, Zhang LF, Wang LN, Guo YK, Cai LH, Yu MM, Wei LH (2011) Highly sensitive and selective fluorescent sensor for Zn^{2+}/

Cu^{2+} and new approach for sensing Cu^{2+} by central metal displacement. Chem Commun 47:5798–5800
20. Jeong YS, Yoon JY (2012) Recent progress on fluorescent chemosensors for metal ions. Inorg Chim Acta 381:2–14
21. Shellaiah M, Wu YH, Singh A, Raju MVR, Lin HC (2013) Novel pyrene- and anthracene-based Schiff base derivatives as Cu^{2+} and Fe^{3+} fluorescence turn-on sensors and for aggregation induced emissions. J Mater Chem A1:1310–1318
22. Li J, Hu Q, Yu X, Zeng Y, Cao C, Liu X, Guo J, Pan Z (2011) A novel rhodamine-benzimidazole conjugate as a highly selective turn-on fluorescent probe for Fe^{3+}. J Fluoresc 21:2005–2013
23. Hu ZQ, Wang XM, Feng YC, Ding L, Li M, Lin CS (2011) A novel colorimetric and fluorescent chemosensor for acetate ions in aqueous media based on a rhodamine 6G–phenylurea conjugate in the presence of Fe(III) ions. Chem Commun 47: 1622–1624
24. Yang Z, Yan C, Chen Y, Zhu C, Zhang C, Dong X, Yang W, Guo Z, Lu Y, He W (2011) A novel terpyridine/benzofurazan hybrid fluorophore: metal sensing behavior and application. Dalton Trans 40:2173–2176
25. Pathak RK, Hinge VK, Mondala P, Rao CP (2012) Ratiometric fluorescence off-on-off sensor for Cu^{2+} in aqueous buffer by a lower rim triazole linked benzimidazole conjugate of calix[4]arene. Dalton Trans 41:10652–10660
26. Singh N, Mulrooney RC, Kaur N, Callan JF (2008) A nanoparticle based chromogenic chemosensor for the simultaneous detection of multiple analytes. Chem Commun 4900–4902
27. Jiang Z, Tang L, Shao F, Zheng G, Lu P (2008) Synthesis and characterization of 9-(cycloheptatrienylidene) fluorene derivatives: new fluorescent chemosensors for detection of Fe^{3+} and Cu^{2+}. Sensors Actuators B 134:414–418
28. Zhao XJ, He RX, Li M, Zhao NW, Li YF, Huang CZ (2013) Formation of blue fluorescent ribbons of 4′,4‴-(1,4-phenylene)bis(2′,:6′,2″-terpyridine) and highly selective visual detection of iron(II) cations. RSC Adv 3:111–116
29. Patil SR, Nandre JP, Jadhav D, Bothra S, Sahoo SK, Devi M, Pradeep CP, Mahulikar PP, Patil UD (2014) Imatinib intermediate as a two in one dual channel sensor for the recognition of Cu^{2+} and I^{-} ions in aqueous media and its practical applications. Dalton Trans. 43: 13299–13306
30. Nandre J, Patil S, Patil V, Yu F, Chen L, Sahoo S, Prior T, Redshaw C, Mahulikar P, Patil U (2014) A novel fluorescent "turn-on" chemosensor for nanomolar detection of Fe(III) from aqueous solution and its application in living cells imaging. Biosens Bioelectron 61:612–617
31. Sharma D, Moirangthem A, Sahoo SK, Basu A, Roy SM, Pati RK, Kumar ASK, Nandred JP, Patil UD (2014) Anion selective chromogenic and fluorogenic chemosensor and its application in breast cancer live cell imaging. RSC Adv 4:41446–41452
32. Chandel M, Roy SM, Sharma D, Sahoo SK, Patel A, Kumari P, Dhale RS, Ashok KSK, Nandre JP, Patil UD (2014) Anion recognition ability of a novel azo dye derived from 4-hydroxycoumarin. J Lumin 154:515–519
33. Sharma D, Sahoo SK, Chaudhary S, Bera RK, Callan JF (2013) Fluorescence 'turn-on' sensor for F^{-} derived from vitamin B6 cofactor. Analyst 138:3646–3650
34. Patil UD, Mahulikar PP (2012) A convenient, $TiCl_4/SnCl_4$ mediated synthesis of *N*-phenyl or *N*-aryl benzamidines and *N*-phenyl picolinamidines. ISRN Organic Chemistry Article ID 963195, 1-6; doi:10.5402/2012/963195
35. Stern O, Volmer M (1919) Uber die abklingungszeit der fluoreszenz. Phys J 20:183–188
36. Schlegel HB, Scuseria GE, Robb MA, Cheeseman JR, Scalmani G, Barone V, Mennucci B, Petersson GA, Nakatsuji H, Caricato M, Li X, Hratchian HP, Izmaylov AF, Bloino F, Zheng G, Sonnenberg GJ, Hada M, Ehara M, Toyota K, Fukuda R, Hasegawa J, Ishida M, Nakajima T, Honda Y, Kitao O, Nakai H, Vreven T, Montgomery JA, Peralta JE, Ogliaro F, Bearpark M, Heyd JJ, Brothers E, Kudin KN, Staroverov VN, Kobayashi R, Normand J, Raghavachari K, Rendell A, Burant JC, Iyengar SS, Tomasi J, Cossi M, Rega N, Millam JN, Klene M, Knox JE, Cross JB, Bakken V, Adamo C, Jaramillo J, Gomperts R, Stratmann RE, Yazyev O, Austin AJ, Cammi R, Pomelli C, Ochterski JW, Martin RL, Morokuma K, Zakrzewski VG, Voth GA, Salvador P, Dannenberg JJ, Dapprich S, Daniels AD, Farkas O, Foresman JB, Ortiz JV, Cioslowski J, Fox DJ (2009) Gaussian 09, revision A.1. Gaussian, Inc., Wallingford